Science of the Total Environment 577 (2017) 236–244

Contents lists available at ScienceDirect

Science of the Total Environment

journal homepage: www.elsevier.com/locate/scitotenv

A novel P/Ag/Ag_2O/Ag_3PO_4/TiO_2 composite film for water purification and antibacterial application under solar light irradiation

Qi Zhu [1], Xiaohong Hu [1], Mishma S. Stanislaus, Nan Zhang, Ruida Xiao, Na Liu, Yingnan Yang *

Graduate School of Life and Environmental Sciences, University of Tsukuba, 1-1-1 Tennoudai, Tsukuba, Ibaraki 305-8577, Japan

HIGHLIGHTS

- P/Ag/Ag_2O/Ag_3PO_4/TiO_2 film showed great photocatalytic ability and stability.
- 10^7 CFU/mL of *E. coli* could be completely inactivated by this film within 5 min.
- Photo-generated holes and $O_2^{\bullet -}$ radicals were the major reactive species.
- This photocatalyst film could be a promising candidate for bacterial disinfection.

GRAPHICAL ABSTRACT

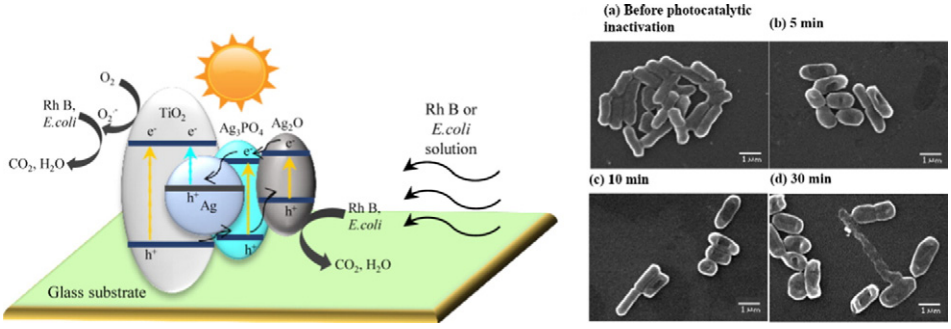

ARTICLE INFO

Article history:
Received 19 July 2016
Received in revised form 20 October 2016
Accepted 21 October 2016
Available online 31 October 2016

Editor: D. Barcelo

Keywords:
P/Ag/Ag_2O/Ag_3PO_4/TiO_2 composite film
Rh B photodegradation
Bacterial inactivation
Photocatalytic mechanism
Simulated solar light irradiation

ABSTRACT

TiO_2-based thin films have been intensively studied in recent years to develop efficient photocatalyst films to degrade refractory organics and inactivate bacteria for wastewater treatment. In the present work, P/Ag/Ag_2O/Ag_3PO_4/TiO_2 composite films on the inner-surface of glass tube were successfully prepared via sol-gel approach. P/Ag/Ag_2O/Ag_3PO_4/TiO_2 composite films with 3 coating layers, synthesized at 400 °C for 2 h, showed the optimal photocatalytic performance for rhodamine B (Rh B) degradation. The results indicated that degradation ratio of Rh B by P/Ag/Ag_2O/Ag_3PO_4/TiO_2 composite film reached 99.9% after 60 min under simulated solar light, while just 67.9% of Rh B was degraded by pure TiO_2 film. Moreover, repeatability experiments indicated that even after five recycling runs, the photodegradation ratio of Rh B over composite film maintained at 99.9%, demonstrating its high stability. Photocatalytic inactivation of *E. coli* with initial concentration of 10^7 CFU/mL also showed around 100% of sterilization ratio under simulated solar light irradiation in 5 min by the composite film. The radical trapping experiments implied that the major active species of P/Ag/Ag_2O/Ag_3PO_4/TiO_2 composite films were photo-generated holes and $O_2^{\bullet -}$ radicals. The proposed photocatalytic mechanism shows that the transfer of photo-induced electrons and holes may reduce the recombination efficiency of electron-hole pairs and potential photo-decomposition of composite film, resulting in enhanced photocatalytic ability of P/Ag/Ag_2O/Ag_3PO_4/TiO_2 composite films.

1. Introduction

As is known to all, water pollution is caused by not only the hazardous chemicals but also pathogenic microorganisms in the world. Therefore, it is very important to disinfect for water purification, because many water

* Corresponding author.
E-mail address: yo.innan.fu@u.tsukuba.ac.jp (Y. Yang).
[1] These authors contributed equally to this work.

http://dx.doi.org/10.1016/j.scitotenv.2016.10.170
0048-9697/

sources are polluted by virus, bacteria and parasitic worm (Mailler et al., 2016; Islam et al., 2015; Sukkasi and Terdthaichairat, 2015; Guerrant et al., 1990; Etchepare et al., 2015; Ortega-Gomez et al., 2016). However, traditional water disinfection methods (such as chlorination and ozonation) have some disadvantages due to the formation of potentially hazardous disinfection byproduct (DBPs) or complicated working to an external device (Bedner and MacCrehan, 2006; Bulloch et al., 2012; Buth et al., 2007; Dodd and Huang, 2007). Recently, photocatalysis has been found as an efficient technology to inactivate bacteria (Gan et al., 2013; Zhu et al., 2012; Thanh-Dong and Lee, 2015; Yu et al., 2016; Pham and Lee, 2015; Hossain et al., 2014; Wang et al., 2013), but more efficient photocatalysts are much needed to develop for water purification.

In our previous study, the solar-light-driven P/Ag/Ag_2O/Ag_3PO_4/TiO_2 photocatalyst was synthesized though sol-gel method, demonstrating extremely high photocatalytic ability and stability for rhodamine B (Rh B, a model of organic waste) degradation under simulated solar light (Hu et al., 2015). However, it was difficult to separate the powder from solution after the photocatalytic reaction, which caused the low efficiency of reusability. As such, it is necessary to improve the reusability efficiency and the possibility of practical application using the effective route, such as coating P/Ag/Ag_2O/Ag_3PO_4/TiO_2 thin film (Lee and Donahue, 2011; Li et al., 2015a). Surprising, there is few report on development of solar-light-driven photocatalyst film on the inner-surface of glass tube for circulatory water purification and antibacterial application. In view of this point, the current study was conducted to prepare P/Ag/Ag_2O/Ag_3PO_4/TiO_2 composite film on the inner-surface of glass tube in order to develop efficient approach for water purification and disinfection. Nowadays there is no report about any investigation of bacterial inactivation by P/Ag/Ag_2O/Ag_3PO_4/TiO_2 photocatalyst. Therefore, it's necessary for us to study sterilization of *E. coli* under solar light irradiation by using P/Ag/Ag_2O/Ag_3PO_4/TiO_2 composite film.

In this study, P/Ag/Ag_2O/Ag_3PO_4/TiO_2 composite film was firstly successfully synthesized by sol-gel method. Then, the influence of synthesis conditions on photocatalytic ability was explored by varying calcination temperature, calcination time and number of coating layers. The structure and optical properties of P/Ag/Ag_2O/Ag_3PO_4/TiO_2 composite films were analyzed, and also the photocatalytic ability of this composite film was investigated through Rh B degradation and sterilization of *E. coli* under solar light irradiation, in comparison with pure TiO_2 film. Further, morphology and microstructure of *E. coli* before and after photocatalytic inactivation were observed using SEM images. Finally, radical trapping experiments were conducted to propose a possible mechanism for Rh B degradation and sterilization of *E. coli* under solar light irradiation.

2. Experiment

2.1. Preparation of P/Ag/Ag_2O/Ag_3PO_4/TiO_2 thin film

All of the reagents purchased from Wako Pure Chemical Industries, Ltd' Japan were of analytical purity. Tetrabutyl titanate ($Ti(OC_4H_9)_4$), ethanol, HNO_3, $AgNO_3$ and Ag_3PO_4 were utilized as TiO_2 source, solvent, dispersing agents and dopants, respectively. Simulated solar light was taken as the irradiation source, and glass tubes (length: 15 cm, φ: 8 mm, Φ: 10 mm) were employed as thin film carrier.

The transparent P/Ag/Ag_2O/Ag_3PO_4/TiO_2 sol was prepared according to our previous study (Hu et al., 2015), and then obtained sol was coated on the inner surface of glass tubes. After coating, the films on glass tubes were dried under 105 °C for 24 h, and then calcined at different temperature ranging from 300 to 500 °C for varied time from 1 to 3 h in the muffle furnace. To prepare 1, 2, 3 and 4-layer films, the processes of coating and drying were repeated several times. Finally, the P/Ag/Ag_2O/Ag_3PO_4/TiO_2 composite films were successfully synthesized.

In order to compare the antibacterial activities between different photocatalysts, Ag, Ag_3PO_4, TiO_2, Ag/TiO_2, Ag_3PO_4/TiO_2 and Ag/Ag_3PO_4 thin films were prepared as controls by the same method. During the synthesis of Ag, Ag_3PO_4 and TiO_2 films, there was just addition of $AgNO_3$, Ag_3PO_4 and tetrabutyl titanate, respectively. For synthesis of Ag/TiO_2, Ag_3PO_4/TiO_2 and Ag/Ag_3PO_4 films, Ag_3PO_4, $AgNO_3$ or TiO_2 were not added, respectively. Certainly, the molar ratio of Ti to Ag was the same as that in P/Ag/Ag_2O/Ag_3PO_4/TiO_2. After the same heat treatments, Ag, Ag_3PO_4, TiO_2, Ag/TiO_2, Ag_3PO_4/TiO_2 and Ag/Ag_3PO_4 thin films were successfully prepared.

2.2. Analytical techniques

The photocatalytic degradation of Rh B was carried out under simulated solar lamp (XC-100, SERIC., Ltd.), and the concentration of Rh B solution was measured by a Shimadzu UV-1600 spectrophotometer. X-ray diffraction (XRD) patterns of thin films were characterized by using a Rigaku Altima III Rint-2000 X-ray diffractometer equipped with Cu Kα radiation (λ = 1.54178 Å). X-ray photoelectron spectra (XPS) were recorded using a Thermo VG Theta Probe (Thermo Fisher SCIENTIFIC), and all of the binding energies were calibrated to the C 1s peak at 284.6 eV. Scanning electron microscopy (SEM, Hitachi FE-SEM S-4800 EDX) was utilized to observe the morphology of thin films. UV–vis diffuse reflectance spectra of different samples were recorded in the range of 200–800 nm on a Shimadzu UV-3100PC Scan UV–vis-NIR spectrometer. The roughness of composite film was measured by AFM (MFP-3D-BIO, Oxford Instruments plc). The leakage of Ag^+ was measured by using a Leeman Prodigy Inductively Coupled Plasma-Optical Emission Spectroscopy (ICP-OES, SPS3520UV-DD) system (SII Nano Technology Inc., Tokyo, Japan).

2.3. Photocatalytic reaction

The photoreaction system consisted of the glass tubes coated thin film, the rotary orbital shaker and simulated solar lamp, with the glass tubes fastened on the shaker. Photocatalytic degradation of Rh B was conducted through glass tubes coated thin films under simulated solar light with 50 mW/cm^2 light intensity, and the initial concentration of Rh B solution was 2 mg/L. The Rh B solution was collected at irradiation time intervals of 30 min, and analyzed to evaluate the concentration of Rh B by a spectrophotometer at a wavelength of 554 nm which corresponds to the maximum absorption wavelength of Rh B molecule.

2.4. Antibacterial activity tests

In this study, XM-G agar medium and Nutrient broth (Japan, BD) were used to isolate and culture the *E. coli*. Phosphate-buffered saline (PBS) (Wako, Japan) was utilized as carrier liquid in this study.

After isolated from Matsumi Lake (University of Tsukuba), *E. coli* was cultured and added into PBS with initial concentration of 10^7 CFU/mL. 50 mL of bacterial liquid was prepared in a beaker which was covered with para-film and used as a supply tank. Then liquid was circulated continuously through the composite film coated glass tube by pump at the flow rate of 24 mL/min. The film coated glass tube with 50.2 cm^2 of reaction surface was irradiated under the simulated solar light with intensity of 50 mW/cm^2. The schematic diagram and the parameters of this tubular cyclic system were shown in Fig. S1.

2.5. Radical trapping experiment

Radical-trapping experiments were conducted to investigate the major active species during the photocatalytic degradation of Rh B over P/Ag/Ag_2O/Ag_3PO_4/TiO_2 composite films. Benzoquinone, ethylenediaminetetraacetate (EDTA) and tBuOH were used as the superoxide anion radical scavenger, hole scavenger and hydroxyl radical scavenger, respectively. Prior to experiments, 1 mM scavenger was added into Rh B solution, and followed by dark condition to reach the adsorption-desorption equilibrium. After irradiation by simulated solar light, the solution was collected at given time intervals, and the concentration of Rh B was measured by a spectrophotometer.

3. Results and discussion

3.1. Optimization of experimental conditions for P/Ag/Ag_2O/Ag_3PO_4/TiO_2 composite film

To investigate optimal calcination conditions for preparing P/Ag/Ag_2O/Ag_3PO_4/TiO_2 composite film, the influences of calcination temperature, calcination time and coating layers were taken into consideration on photocatalytic ability as shown in Fig. 1. Firstly, P/Ag/Ag_2O/Ag_3PO_4/TiO_2 composite films were prepared under calcination varying from 300 °C to 500 °C for 2 h, respectively, and Rh B molecule was chosen as the model pollutant to evaluate the photocatalytic activities of composite films under simulated solar light (50 mW/cm^2 illumination intensity). It can be found that photocatalytic activities were significantly influenced by calcination temperature. The Rh B degradation efficiency of P/Ag/Ag_2O/Ag_3PO_4/TiO_2 composite film increased from 83.9% to 99.9% with calcination temperature increased from 300 to 400 °C (Fig. 1a_1). Then degradation ratio reached the maximum at 400 °C, while it largely decreased to 82.1% with temperature further increased to 500 °C. This result was mainly caused by the changes of crystal phases (Shang et al., 2011; Peng et al., 2015). The XRD patterns of as-prepared films (400 °C and 500 °C) were well in accord with anatase (JCPDS file no.00-021-1272). It can be found (Fig. 1b_1) that the anatase phase appeared and increases once the calcination temperature increase from 300 °C to 400 °C, resulting in the increase photocatalytic performance. However, more rutile phase is transferred from anatase phase under temperature higher than 400 °C, leading to the decrease of photocatalytic ability, because anatase phase has higher photocatalytic activity than rutile phase (Peng et al., 2015; Carp et al., 2004; Mandal and Bhattacharyya, 2012). Meanwhile, the peak of metallic Ag (JCPDS file no.01-071-3762) was observed at 400 °C, which proved the existence of metallic Ag in the composite film. However, the main diffraction peak of Ag at 38.2° was not independently observed due to the significant overlap with the peak at 37.8° ascribed to the (004) plane of anatase TiO_2 (Aazam, 2014). Stronger peaks at 37.8°, 44.3° and 64.5°ascribed to the (110), (200) and (220) planes of metallic silver at 500 °C resulted from higher crystallinity of Ag nanoparticles (Kuo et al., 2016). Apart from XRD result, the strongest light absorption

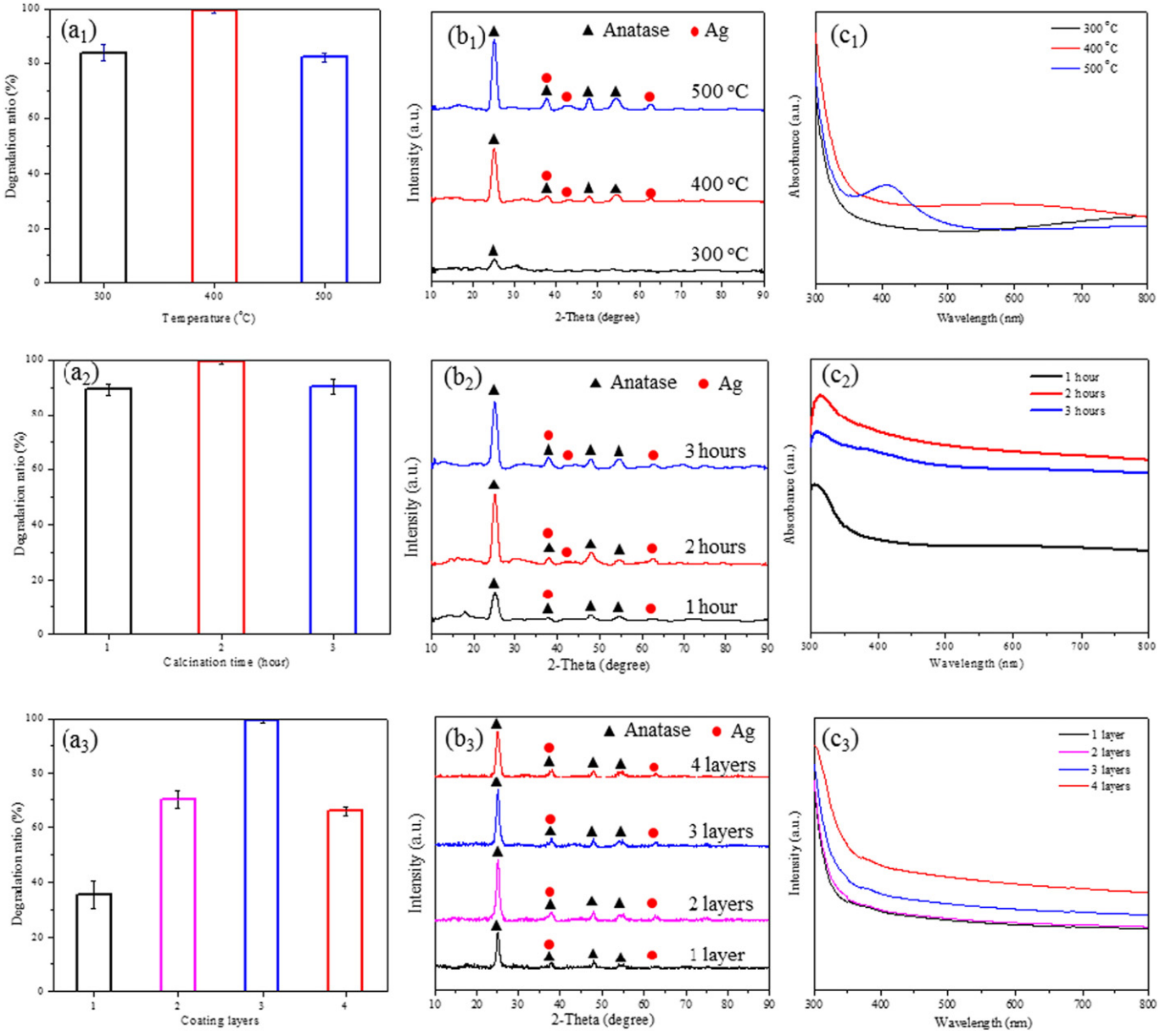

Fig. 1. Influences of calcination temperature, calcination time and coating layers on (a_{1-3}) photocatalytic Rh B degradation, (b_{1-3}) XRD patterns and (c_{1-3}) UV–vis spectra of P/Ag/Ag_2O/Ag_3PO_4/TiO_2 composite films, respectively.

band around 450–800 nm at 400 °C (Fig. 1c$_1$) also contributed to its highest photocatalytic ability, compared with 300 °C and 500 °C. It should be noted that the composite film (500 °C) exhibited a single absorption peak centered at 400 nm in Fig. 1c$_1$, due to the surface plasmon resonance (SPR) of Ag nanoparticles (Akhavan, 2009; Zhu et al., 2015; Leong et al., 2014), which agreed well with XRD results.

The effects of calcination time on photocatalytic activity were further investigated by the composite films, which were calcinated under the optimal calcination temperature of 400 °C for 1, 2 and 3 h, respectively. The results demonstrated that the removal efficiency reached highest via films calcinated for 2 h (Fig. 1a$_2$), which mainly due to the varied content of anatase and metallic silver. As shown in Fig. 1b$_2$, the stronger intensity of anatase in 2-h than 1-h XRD pattern demonstrated more content of anatase phase, which could lead to higher photocatalytic ability. However, 3-h calcination did not cause much higher photocatalytic activity, maybe because more content of silver could provide more recombination sites for photogenerated electrons and holes (Mohamed and Al-Sharif, 2013; Hájková et al., 2014), inhibiting the generation of active free radicals. Besides, 2-h composite film showed the highest light absorption in the range of 300–800 nm (Fig. 1c$_2$). These results indicated that appropriate calcination for P/Ag/Ag_2O/Ag_3PO_4/TiO_2 composite film was 400 °C for 2 h.

In addition, coating layers of films affected its photocatalytic performance, and the results were shown in Fig. 1a$_3$–c$_3$. It could be seen that 3-layer film showed the highest Rh B degradation performance, in comparison with 1-layer, 2-layer and 4-layer films, which may be ascribed to the appropriate thickness of film on the inner surface of glass tubes. XRD patterns proved that 1-layer film showed lower intensity compared to other films. Besides, 1-layer and 2-layer films obviously exhibited lower UV–vis spectra in comparison with 3-layer and 4-layer films, due to their thinner thickness. As widely recognized, during photocatalytic reaction, Rh B molecules were firstly adsorbed on the solid-liquid inter-surface of films, meanwhile the photocatalyst film was under light irradiation, so the Rh B molecule could be degraded by photo-induced free radicals (Dong et al., 2010; Li et al., 2013; Teng et al., 2012). Although 4-layer film with large thickness could provide sufficient sites for adsorbing Rh B molecular, thicker film could block the light irradiation, which may be the reasons that 3-layer film exhibited the greatest photodegradation performance.

3.2. Comparison of as-prepared TiO_2 and P/Ag/Ag_2O/Ag_3PO_4/TiO_2 composite films and repetitive experiments

The P/Ag/Ag_2O/Ag_3PO_4/TiO_2 composite films were prepared under optimal condition. According to SEM results (Fig. S2), composite film coated on glass is not continuous after calcination at 400 °C for 2 h. However, this composite film after calcination showed the highest photocatalytic efficiency. Therefore, discontinues photocatalyst film still has exactly high photocatalytic activity. It could be clearly observed in Fig. S3 that many particles have been successfully located on the surface of TiO_2, indicating P/Ag/Ag_2O/Ag_3PO_4/TiO_2 composite film has been successfully prepared. Besides, thickness, roughness and mass of immobilized catalyst have also been investigated, respectively. The results indicated that thickness of composite film (Fig. S4) was about 405 ± 6 nm, and its roughness was 70.833 nm measured by AFM. Mass of immobilized catalyst was 0.13 g/tube. Compared with pure TiO_2 films, the prepared P/Ag/Ag_2O/Ag_3PO_4/TiO_2 composite films showed enhanced photocatalytic degradation efficiency (Fig. S5a). Rh B molecule was almost completely degraded by the P/Ag/Ag_2O/Ag_3PO_4/TiO_2 composite film after 60 min irradiation. However, only 69.7% of Rh B molecules were removed over pure TiO_2 films. The enhanced photocatalytic abilities of P/Ag/Ag_2O/Ag_3PO_4/TiO_2 composite films mainly owe to much higher absorption in the range from 300 nm to 800 nm as shown in Fig. S5b, compared to TiO_2 films. This enhanced absorption is mainly due to the introduction of metallic Ag, Ag_2O and Ag_3PO_4 semiconductors (Viana et al., 2013; Li et al., 2014; Bu et al., 2015). All of metallic Ag, Ag_2O and Ag_3PO_4 semiconductors can be excited by visible light and the band gap of Ag_2O and Ag_3PO_4 are 1.2 eV and 2.5 eV, respectively (Wang et al., 2011; Cao et al., 2012). Moreover, the band gap of P/Ag/Ag_2O/Ag_3PO_4/TiO_2 composite was calculated about 2.2 eV in our previous study (Hu et al., 2015), which is much smaller than that of pure TiO_2 (3.2 eV) (Savio et al., 2016). More importantly, surface plasmon resonance (SPR) of metallic Ag has reportedly been investigated affecting the light absorption, and resulting in the strong absorption band from 400 nm to 800 nm (Kamimura et al., 2016). Furthermore, the crystallite size of P/Ag/Ag_2O/Ag_3PO_4/TiO_2 composite film (4.8 nm) calculated by Halder-Wagner method was smaller than pure TiO_2 film (5.8 nm), which may be the one of reasons for its good photocatalytic ability, because smaller crystallite size usually results from the transformation of rutile phase to anatase phase (Xin et al., 2015; Šuligoj et al., 2016). P/Ag/Ag_2O/Ag_3PO_4/TiO_2 composite films also had rougher surfaces than pure TiO_2 films as shown in Fig. S3. Therefore, stronger absorption in visible light region, smaller band gap and smaller crystallite size could contribute to its improved photocatalytic ability compared to pure TiO_2 films.

Furthermore, we conducted the repeatability experiments through Rh B degradation to evaluate the photocatalytic stability of P/Ag/Ag_2O/Ag_3PO_4/TiO_2 composite films, and the results were shown in Fig. 2a. It

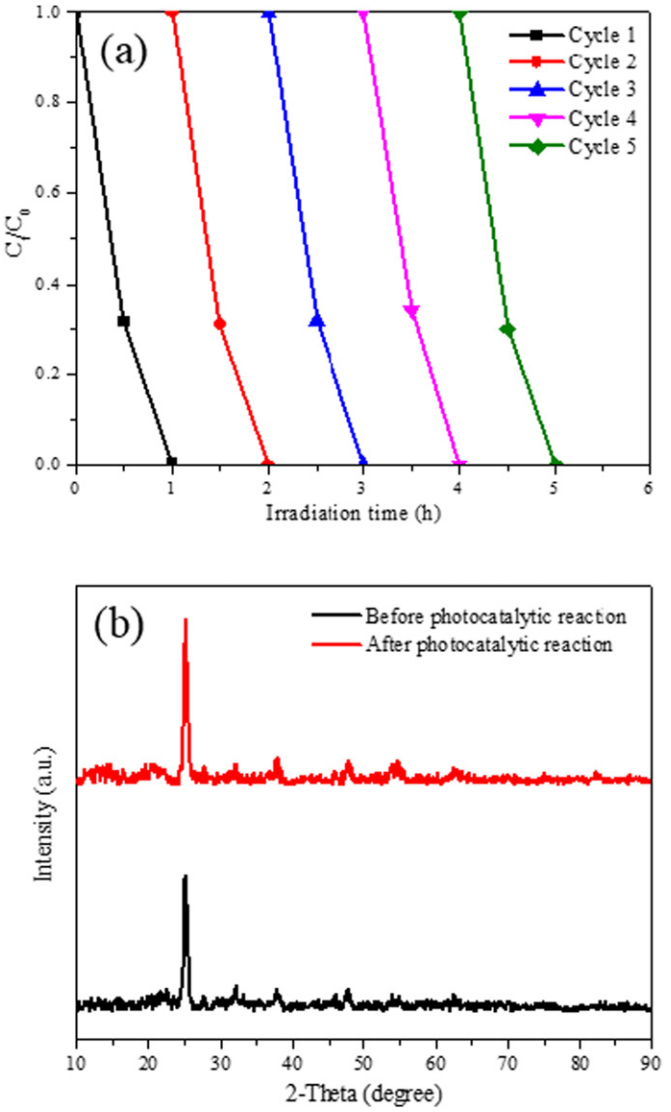

Fig. 2. (a) Repetitive performance of P/Ag/Ag_2O/Ag_3PO_4/TiO_2 composite films for Rh B degradation; (b) XRD patterns of P/Ag/Ag_2O/Ag_3PO_4/TiO_2 composite films before and after photocatalytic reaction.

could be found that after five recycling runs, the photodegradation ratio of Rh B over P/Ag/Ag_2O/Ag_3PO_4/TiO_2 composite film was still at 99.9%, indicating its exactly high photocatalytic stability. Also, XRD patterns (Fig. 2b) showed that there were almost no changes between P/Ag/Ag_2O/Ag_3PO_4/TiO_2 composite films before and after photocatalytic reaction. After five-circle photocatalytic reaction, P/Ag/Ag_2O/Ag_3PO_4/TiO_2 composite film still exhibited clear and strong peaks at 25.28°, 37.80° and 48.05°, which are ascribed to (101), (112) and (200) planes of anatase phase, respectively (Sofianou et al., 2015; Wang et al., 2016). Equally importantly, there was almost no Ag^+ leaked from P/Ag/Ag_2O/Ag_3PO_4/TiO_2 composite film after 90 min irradiation (not shown). All of these results demonstrated that P/Ag/Ag_2O/Ag_3PO_4/TiO_2 composite film possess exactly high photocatalytic stability, which is in favor of its practical application in wastewater treatment.

3.3. Chemical composition of P/Ag/Ag_2O/Ag_3PO_4/TiO_2 thin films

To analyze the surface element composition and chemical state for P/Ag/Ag_2O/Ag_3PO_4/TiO_2 composite film, X-ray photoelectron spectra (XPS) was used and the results were shown in Fig. 3. It could be found in Ag 3d XPS spectra (Fig. 3a) that the peaks located at 373.5 eV and 367.5 eV are ascribed to the Ag $3d_{3/2}$ and Ag $3d_{5/2}$ binding energies, each of which could be further divided into two peaks at 373.5 eV, 374.4 eV and 367.5 eV, 368.4 eV, respectively (Tian et al., 2012; Guo et al., 2013). The peaks at 374.4 eV and 368.4 eV are assigned to metallic Ag^0, while those at 373.5 eV and 367.5 eV are attributed to the Ag^+. The broad O 1s region of P/Ag/Ag_2O/Ag_3PO_4/TiO_2 was fitted by four peaks (Fig. 3b). The major peak at 530.2 eV is attributed to lattice oxygen (Ti—O), while the peaks at 532.0 eV and 534.0 eV correspond to oxygen of surface OH bound in —Ti(OH)—O—Ti(OH)— and oxygen of water molecules, respectively (Akhavan, 2009). Besides, the peaks located at 529.3 eV (Fig. 3b) proved the existence of Ag_2O in composite film, which was in accord with our previous study (Hu et al., 2015). Interestingly, Ag_2O also has high photocatalytic activity under visible light, and the introduction of Ag_2O could improve the photocatalytic ability for this composite film (Yu et al., 2005). As can be seen from Fig. 3c that the peak centered at 133.4 eV belongs to P 2p, which demonstrated phosphorus existed in a pentavalent-oxidation state (P^{5+}) (Méndez et al., 2005). According to our previous TEM analysis (Hu et al., 2015), Ag_3PO_4 also was successfully formed in the composite during the calcination. Therefore, this composite thin film consisted of nonmetal P, metallic Ag, Ag_2O, Ag_3PO_4 and TiO_2. This composite film could have enhanced photocatalytic ability, because all of Ag, Ag_2O and Ag_3PO_4 have good ability under visible light.

3.4. Photocatalytic inactivation of E. coli by thin film coated tubular cyclic system

P/Ag/Ag_2O/Ag_3PO_4/TiO_2 composite film coated tubular cyclic system was developed as the reactor system for *E. coli* inactivation (Fig. S1). *E. coli* inactivation by photocatalyst composite films with and without irradiation was shown in Fig. 4 using tubular cyclic system. The results showed that almost 100% of *E. coli* with initial concentration of 10^7 CFU/mL was damaged by P/Ag/Ag_2O/Ag_3PO_4/TiO_2 composite film in only about 5 min of irradiation, while it took 10 min in dark condition. However, there was almost no effect of pure TiO_2 film on *E. coli* inactivation. It also can be seen from Fig. 5a that *E. coli* cultured without any photocatalyst showed many colonies, and colonies of *E. coli* cultured over pure TiO_2 film decreased little under the solar light (Fig. 5b). Fig. 5c illustrated the *E. coli* cultured on composite film in the dark, which showed much less colonies than that cultured with pure TiO_2 film under solar light. However, there was no colony observed on composite film after 5 min irradiation (Fig. 5d). In conclusion, this composite photocatalyst film showed extremely high efficiency for *E. coli* inactivation with and without light irradiation, in comparison of pure TiO_2 film. In order to compare with P/Ag/Ag_2O/Ag_3PO_4/TiO_2 composite film, Ag film, Ag_3PO_4 film, Ag/TiO_2 film, Ag_3PO_4/TiO_2 film and Ag/Ag_3PO_4 film were synthesized as controls. The repetitive experiments in Fig. S6 indicated that P/Ag/Ag_2O/Ag_3PO_4/TiO_2 composite film still exhibited exactly high efficiency for *E.coli* inactivation (initial concentration: 10^7 CFU/mL) at the third cycle (5 min per cycle). However, photocatalytic activities of Ag film, Ag_3PO_4 film and Ag/Ag_3PO_4 film largely decreased after one-cycle experiment. Although Ag/TiO_2 film and Ag_3PO_4/TiO_2 film had photocatalytic stability, their photocatalytic efficiencies for *E.coli* inactivation were much lower than that of P/Ag/Ag_2O/Ag_3PO_4/TiO_2 composite film. Therefore, P/Ag/Ag_2O/Ag_3PO_4/TiO_2 composite film not only has high photocatalytic activity, but also has remarkable photocatalytic stability.

SEM images were used to analyze the morphology and microstructure of *E. coli* before and after photocatalytic inactivation (Fig. 6a–d). Before photocatalytic treatment, *E. coli* cell had an intact cell structure and a smooth surface (Fig. 6a). But only after 5 min of photocatalytic inactivation, the surface of the cell obviously became abnormal, and some pits and holes can be observed on the membrane of *E. coli* (Fig. 6b), which was consistent with previous results (Fig. 4). Results also showed that *E. coli* was treated by P/Ag/Ag_2O/Ag_3PO_4/TiO_2 composite film for 10 min irradiation (Fig. 6c), forming bigger pits and holes in their cell walls. Future, *E. coli* was deeply damaged after 30 min of photocatalytic inactivation with much rougher surface, and some materials inside cell were even lost (Fig. 6d). According to reported study (Li et al., 2015b), it was for 4 h that *E. coli* could be obviously damaged by g-C_3N_4/TiO_2 under visible light. Those results indicated that P/Ag/Ag_2O/Ag_3PO_4/TiO_2 composite film exhibited extremely high photocatalytic inactivation efficiency, and only 5 min of solar light irradiation led to the destruction of *E. coli* structure.

In this study, silver and silver salt (Ag_2O and Ag_3PO_4) plays important roles for enhancing photocatalytic activity (Hu et al., 2015). They could decrease the original band gap to improve its photocatalytic efficiency under visible light. However, during the photocatalytic treatment by some other photocatalysts doped with silver salt, the Ag^+ may leak

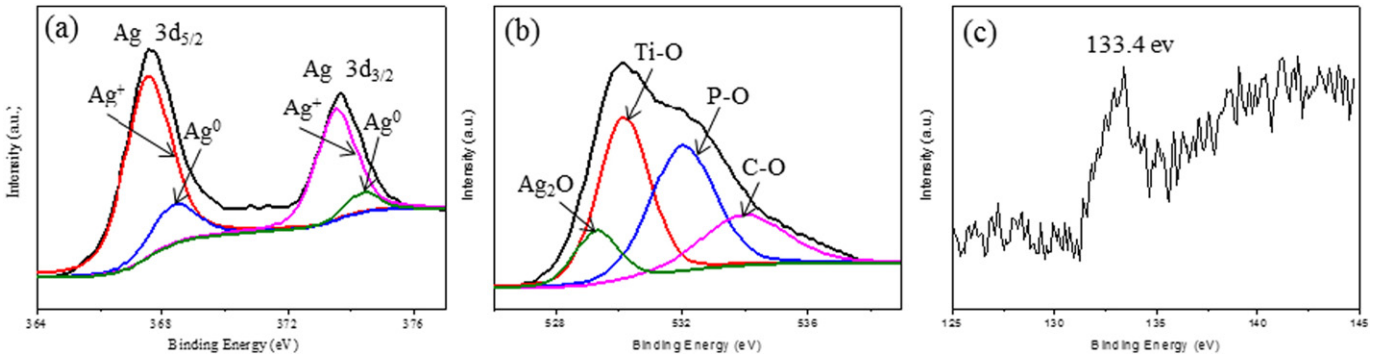

Fig. 3. (a) Ag 3d, (b) O 1s and (c) P 2p X-ray photoelectron spectra for P/Ag/Ag_2O/Ag_3PO_4/TiO_2 composite films.

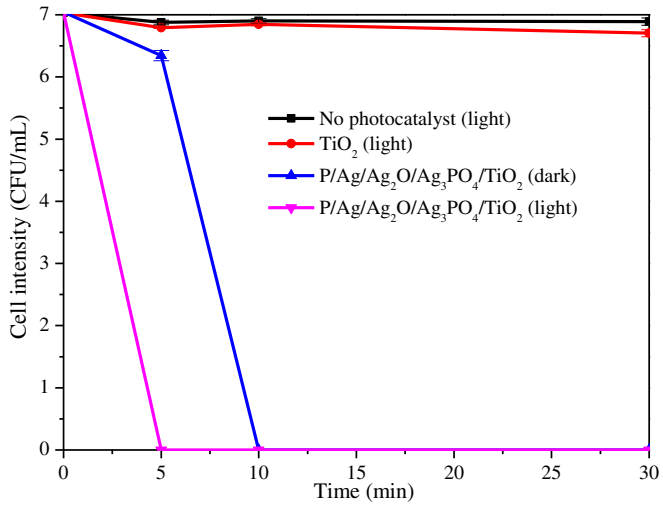

Fig. 4. Disinfection rate of *E.coli* in control, TiO_2 and P/Ag/Ag_2O/Ag_3PO_4/TiO_2 under different irradiation conditions in 30 min by thin film coated tubular cyclic system.

to the aqueous solution, and excess of silver ion is harmful to the health (Ng et al., 2016).

Therefore, photocatalytic stability is also an important aspect for practical application. In this work, the leakage of Ag^+ was measured after the photocatalytic reaction, and the leakage of silver ion from P/Ag/Ag_2O/Ag_3PO_4/TiO_2 powder and thin film were kept in the range of 0–0.02 mg/L. Based on the safety standard value of less than 0.1 mg/L from WHO (Wang and Lim, 2013), this composite photocatalytic could be an appropriate candidate for practical application because it meets the safety standard of WHO.

In order to further investigate the photocatalytic ability of this novel composite film, photocatalytic inactivation ratio of *E. coli* by P/Ag/Ag_2O/Ag_3PO_4/TiO_2 composite film was calculated in comparison of other reported photocatalyst films, such as TiO_2/In_2O_3 (Petronella et al., 2014), PdO-TiO_2 (Erkan et al., 2006) and TiO_2 (Dheaya et al., 2009; Kim et al., 2013). All of their experimental parameters were listed in Table 1. It could be found that P/Ag/Ag_2O/Ag_3PO_4/TiO_2 composite film showed the highest ability, and its photocatalytic inactivation ratio reached to 1.99×10^6 CFU/(cm^2·min) under solar light. However, reported pure TiO_2 films showed 222 CFU/(cm^2·min) (Petronella et al., 2014) and 4.66×10^5 CFU/(cm^2·min) (Erkan et al., 2006) under UV light,

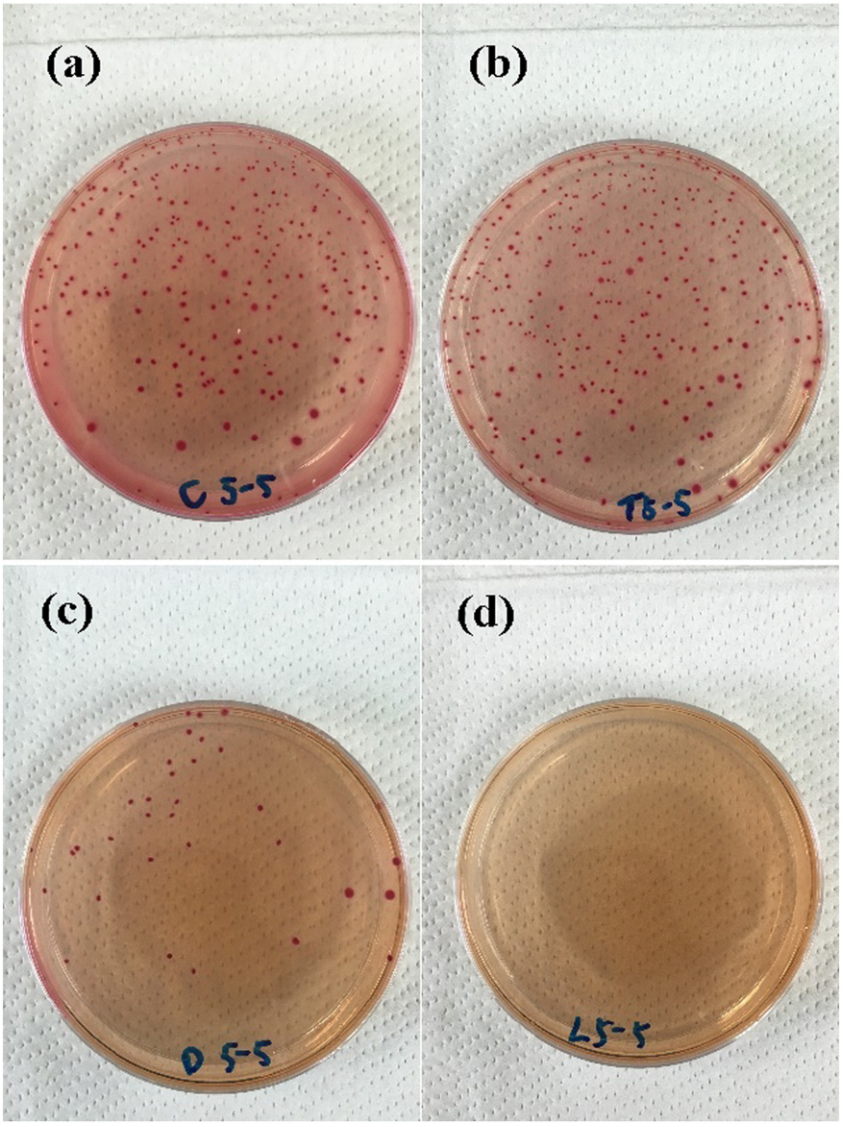

Fig. 5. Colonies of *E.coli* cultured for 5 min with initial concentration of 10^7 CFU/mL (a) without photocatalyst film, (b) over pure TiO_2 film under solar light, (c) on P/Ag/Ag_2O/Ag_3PO_4/TiO_2 composite film in the dark, and (d) on P/Ag/Ag_2O/Ag_3PO_4/TiO_2 composite film under solar light.

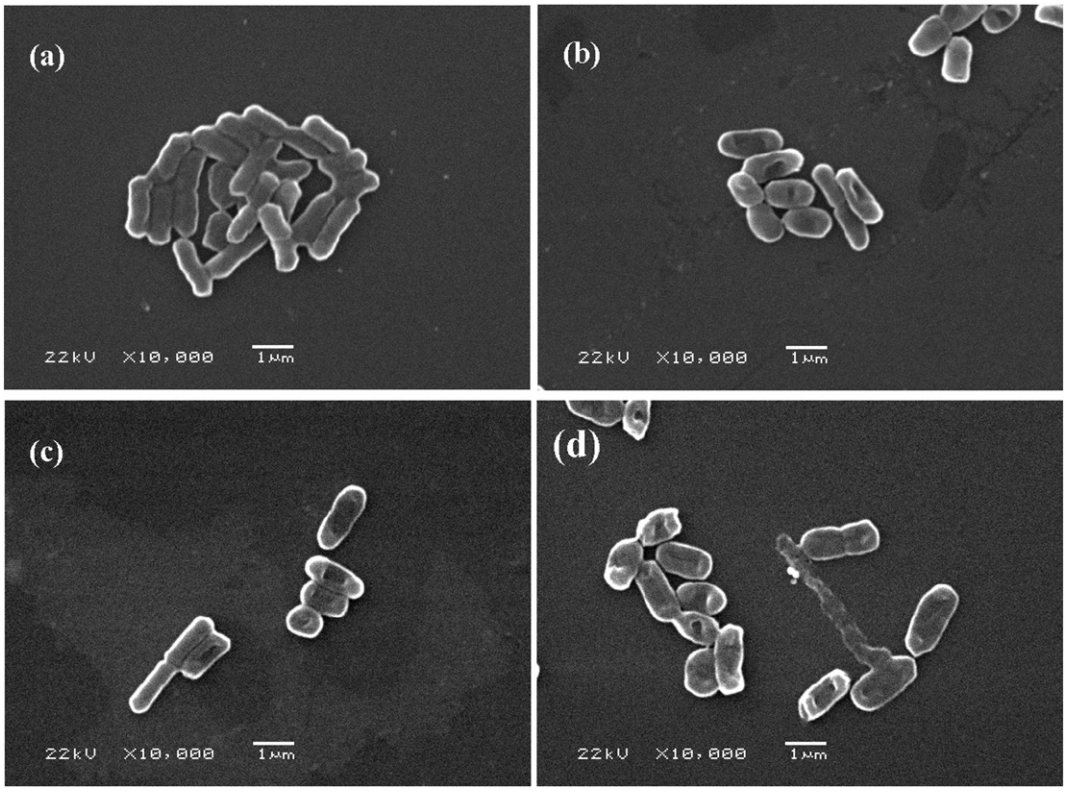

Fig. 6. SEM observation of *E.coli* (a) before photocatalytic inactivation, (b) after 5 min, (c) 10 min and (d) 30 min of photocatalytic inactivation by P/Ag/Ag_2O/Ag_3PO_4/TiO_2 composite film.

respectively. TiO_2/In_2O_3 and PdO-TiO_2 exhibited 555 and 0.08 CFU/(cm^2·min), respectively (Dheaya et al., 2009; Kim et al., 2013). Therefore, our novel composite film showed higher efficiency more over 3000 times than reported PdO-TiO_2 film under solar light irradiation. These results concluded that as-prepared P/Ag/Ag_2O/Ag_3PO_4/TiO_2 composite film exhibited the great potential for sterilization due to its low cost, high efficiency and environment friendly. And this work laid an important foundation for the development and application of water purification and bacterial disinfection system.

3.5. Mechanism of photocatalytic activity for P/Ag/Ag_2O/Ag_3PO_4/TiO_2 thin films

To understand the role of active radicals during photocatalytic process, radical trapping experiments were performed by using P/Ag/Ag_2O/Ag_3PO_4/TiO_2 composite films (Fig. S7) (Cao et al., 2013; Kim et al., 2010). As can be seen, compared to the control (without scavengers), Rh B degradation efficiency only decreased around 2.7% after 1 h of irradiation by injection of hydroxyl radical scavenger (1 mM *t*BuOH). However, photocatalytic efficiency was largely inhibited by a hole scavenger (1 mM EDTA), and only 40.9% Rh B molecules were decomposed after 1 h of irradiation. The addition of superoxide anion radical scavenger (1 mM benzoquinone) resulted in the reduction of photocatalytic efficiency, with 73.7% degradation ratio in 1 h. These results indicated that hydroxyl radical play less important role on Rh B photocatalytic degradation, but holes and superoxide anion radicals are the primary active species during photocatalytic process. This result is consistent with our previous study (Hu et al., 2015).

On the basis of the above results, the photocatalytic mechanism of P/Ag/Ag_2O/Ag_3PO_4/TiO_2 composite film for Rh B degradation and *E. coli* inactivation was discussed and its illustration was shown in Fig. 7. Firstly, Rh B molecules and *E. coli* cells are adsorbed on the surface of P/Ag/Ag_2O/Ag_3PO_4/TiO_2 composite film, and then the adsorbed Rh B molecules and *E. coli* cells are decomposed by photogenerated active species on composite film surfaces. Hence, the possible pathways for generating active species are proposed following (Hu et al., 2015; Wang et al., 2011; Cao et al., 2012; Zielinska-Jurek et al., 2011). As Ag_3PO_4, Ag_2O and TiO_2 can be excited under simulated solar light irradiation, their photogenerated electrons are excited from valence bands to the conduction bands, and holes stay at valence bands. Then the excited electrons on the conduction band of Ag_2O (0.2 eV vs. NHE) and Ag_3PO_4 (0.45 eV vs. NHE) could flow to the Fermi level of Ag (0.99 eV vs. NHE). While photo-generated holes at valence bands of TiO_2 and Ag_3PO_4 could transfer to Ag_2O. As a consequence, this transfer of photo-generated electrons and holes could decrease the possibility of their recombination, leading to enhanced photocatalytic ability. Moreover, excitation of surface plasmon resonance (SPR) from the plasmonic-metal Ag could lead to generation of energetic electrons, which can be directly injected to the TiO_2 surface (Cao et al., 2013). Then photo-generated electrons on the TiO_2 interface could react with oxygen (O_2) to generate superoxide

Table 1
Inactivation ratio of P/Ag/Ag_2O/Ag_3PO_4/TiO_2 film compared with different photocatalyst films (Ng et al., 2016; Wang and Lim, 2013; Petronella et al., 2014; Erkan et al., 2006).

Photocatalyst	Initial concentration (CFU/mL)	Solution value (mL)	Inactivation ratio (%)	Surface area (cm^2)	Inactivation time (min)	Inactivation rate (CFU/(cm^2·min))	Reference
P/Ag/Ag_2O/Ag_3PO_4/TiO_2 (solar light)	10^7	50	99.999	50.2	5	1.99×10^6	This study
TiO_2/In_2O_3 (solar light)	10^7	0.02	99.9	4	90	555	(Ng et al., 2016)
PdO-TiO_2 (UV)	10^3	0.2	99.9	19	120	0.08	(Wang and Lim, 2013)
TiO_2 (UVA)	$2 \cdot 10^3$	567	99.9	56.72	90	222	(Petronella et al., 2014)
TiO_2 (UV)	10^6	3000	99.9	644.3	10	4.66×10^5	(Erkan et al., 2006)

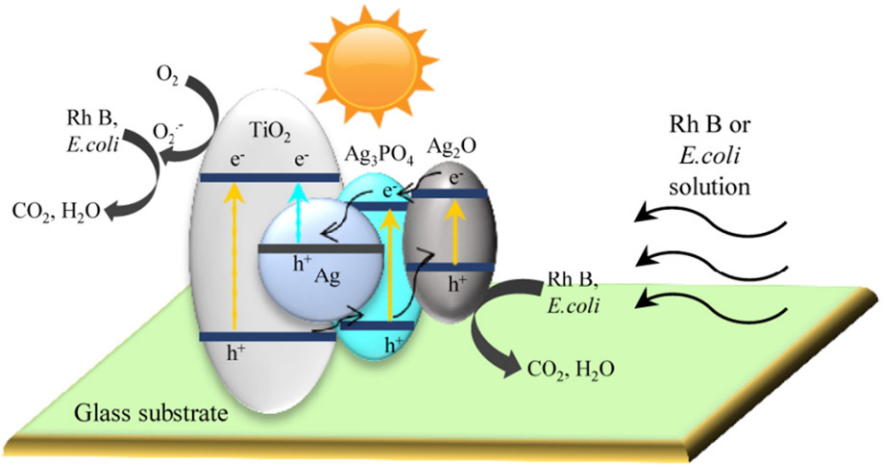

Fig. 7. Photocatalytic mechanism of P/Ag/Ag_2O/Ag_3PO_4/TiO_2 composite film under simulated solar light. (↑: excitation of solar light; ↑: excitation of SPR; ⌒: charge transfer).

anion radicals ($O_2^{\bullet-}$). Superoxide anion radicals and generated holes can directly decompose adsorbed Rh B molecules and *E. coli* cells on the composite films, which have been proved by radial trapping experiments.

More importantly, the high photostability of P/Ag/Ag_2O/Ag_3PO_4/TiO_2 composite film could be well explained by above mentioned mechanism. One of reasons is that Ag_3PO_4 can be protected from photodecomposition through transferring photo-excited electrons and holes to Ag and Ag_2O, respectively. Also, Ag could act as an electron acceptor to hinder the recombination of electron-hole pairs of Ag_2O and Ag_3PO_4, enhancing the photocatalytic ability. What is more, the structure stability of Ag_2O can be well maintained in the presence of metallic Ag by the self-stability mechanism (Wang et al., 2011). As a consequence, the structure stability of Ag_2O and Ag_3PO_4 prevent the Ag^+ leakage from composite films and maintain the structure stability of composite films.

4. Conclusions

In summary, the P/Ag/Ag_2O/Ag_3PO_4/TiO_2 composite films were successfully prepared under optimal experimental conditions by sol-gel method. P/Ag/Ag_2O/Ag_3PO_4/TiO_2 composite films exhibited much higher photocatalytic ability on photocatalytic organic degradation and sterilization than pure TiO_2 films, as the composite films possessed smaller crystallite size, smaller grain size, and stronger absorption in visible light region. More importantly, P/Ag/Ag_2O/Ag_3PO_4/TiO_2 composite films showed consistent stability, which benefited from the charge transfer within the composite structure and the self-stability mechanism. The excellent photocatalytic performance of P/Ag/Ag_2O/Ag_3PO_4/TiO_2 composite films was attributed to the synergistic effect of these factors. In comparison with other reported photocatalyst films, P/Ag/Ag_2O/Ag_3PO_4/TiO_2 composite film exhibited extremely high sterilization efficiency under solar light irradiation. Therefore, P/Ag/Ag_2O/Ag_3PO_4/TiO_2 composite film could be a promising candidate for its practical applications in environmental purification and sterilization, due to its high photocatalytic ability and stability.

Acknowledgements

This work is supported by Grant-in-Aid for Exploratory Research 26670901 and Scientific Research (B) 15H02859 from Japan Society for the Promotion of Science (JSPS).

Appendix A. Supplementary data

Supplementary data to this article can be found online at http://dx.doi.org/10.1016/j.scitotenv.2016.10.170.

References

Aazam, E.S., 2014. Visible light photocatalytic degradation of thiophene using Ag–TiO_2/multi-walled carbon nanotubes nanocomposite. Ceram. Int. 40 (5), 6705–6711.
Akhavan, O., 2009. Lasting antibacterial activities of Ag–TiO_2/Ag/a-TiO_2nanocomposite thin film photocatalysts under solar light irradiation. J. Colloid Interface Sci. 336 (1), 117–124.
Bedner, M., MacCrehan, W.A., 2006. Transformation of acetaminophen by chlorination produces the toxicants 1,4-benzoquinone and *N*-acetyl-p-benzoquinoneimine. Environ. Sci. Technol. 40 (2), 516–522.
Bu, Y., Chen, Z., Sun, C., 2015. Highly efficient *Z*-Scheme Ag_3PO_4/Ag/WO_{3-x} photocatalyst for its enhanced photocatalytic performance. Appl. Catal. B Environ. 179, 363–371.
Bulloch, D.N., Lavado, R., Forsgren, K.L., Beni, S., Schlenk, D., Larive, C.K., 2012. Analytical and biological characterization of halogenated gemfibrozil produced through chlorination of wastewater. Environ. Sci. Technol. 46 (10), 5583–5589.
Buth, J.M., Arnold, W.A., McNeill, K., 2007. Unexpected products and reaction mechanisms of the aqueous chlorination of cimetidine. Environ. Sci. Technol. 41 (17), 6228–6233.
Cao, J., Luo, B., Lin, H., Xu, B., Chen, S., 2012. Visible light photocatalytic activity enhancement and mechanism of AgBr/Ag_3PO_4 hybrids for degradation of methyl orange. J. Hazard. Mater. 217, 107–115.
Cao, J., Zhao, Y., Lin, H., Xu, B., Chen, S., 2013. Facile synthesis of novel Ag/AgI/BiOI composites with highly enhanced visible light photocatalytic performances. J. Solid State Chem. 206, 38–44.
Carp, O., Huisman, C.L., Reller, A., 2004. Photoinduced reactivity of titanium dioxide. Prog. Solid State Chem. 32, 33–177.
Dheaya, M.A.A., Patrick, S.M.D., Trudy, A.M., Byrne, J.A., 2009. Photocatalytic inactivation of *E. coli* in surface water using immobilised nanoparticle TiO_2 films. Water Res. 43, 47–54.
Dodd, M.C., Huang, C.-H., 2007. Aqueous chlorination of the antibacterial agent trimethoprim: reaction kinetics and pathways. Water Res. 41 (3), 647–655.
Dong, W., Lee, C.W., Lu, X., 2010. Synchronous role of coupled adsorption and photocatalytic oxidation on ordered mesoporous anatase TiO_2–SiO_2nanocomposites generating excellent degradation activity of RhB dye. Appl. Catal. B Environ. 95 (3), 197–207.
Erkan, A., Bakir, U., Karakas, G., 2006. Photocatalytic microbial inactivation over Pd doped SnO_2 and TiO_2 thin films. J. Photochem. Photobiol. A Chem. 184, 313–321.
Etchepare, R., Zaneti, R., Azevedo, A., Rubio, J., 2015. Application of flocculation-flotation followed by ozonation in vehicle wash wastewater treatment/disinfection and water reclamation. Desalin. Water Treat. 56, 1728–1736.
Gan, H., Zhang, G., Huang, H., 2013. Enhanced visible-light-driven photocatalytic inactivation of *Escherichia coli* by $Bi_2O_2CO_3$/Bi_3NbO_7 composites. J. Hazard. Mater. 250–251, 131–137.
Guerrant, R.L., Hughes, J.M., Lima, N.L., Crane, J., 1990. Diarrhea in developed and developing-countries – magnitude, special settings, and etiologies. Rev. Infect. Dis. 12, S41–S50.
Guo, J., Ouyang, S., Zhou, H., Kako, T., Ye, J., 2013. Ag_3PO_4/$In(OH)_3$ Composite photocatalysts with adjustable surface-electric property for efficient photodegradation of organic dyes under simulated solar-light irradiation. J. Phys. Chem. C 117, 17716–17724.
Hájková, P., Matoušek, J., Antoš, P., 2014. Aging of the photocatalytic TiO_2 thin films modified by Ag and Pt. Appl. Catal. B Environ. 160, 51–56.
Hossain, F., Perales-Perez, O.J., Hwang, S., Román, F., 2014. Antimicrobial nanomaterials as water disinfectant: applications, limitations and future perspectives. Sci. Total Environ. 466–467, 1047–1059.
Hu, X., Zhu, Q., Wang, X., Kawazoe, N., Yang, Y., 2015. Nonmetal–metal–semiconductor-promoted P/Ag/Ag_2O/Ag_3PO_4/TiO_2 photocatalyst with superior photocatalytic activity and stability. J. Mater. Chem. A 3 (34), 17858–17865.
Islam, M.A., Azad, A.K., Akber, M.A., Rahman, M., Sadhu, I., 2015. Effectiveness of solar disinfection (SODIS) in rural coastal Bangladesh. J. Water Health 13, 1113–1122.
Kamimura, S., Miyazaki, T., Zhang, M., Li, Y., Tsubota, T., Ohno, T., 2016. (Au@Ag)@Au double shell nanoparticles loaded on rutile $TiO_2$for photocatalytic decomposition of 2-propanol under visible light irradiation. Appl. Catal. B Environ. 180, 255–262.

Kim, J., Lee, C.W., Choi, W., 2010. Platinized WO_3 as an Environmental Photocatalyst that Generates OH Radicals under Visible Light. Environ. Sci. Technol. 44, 6849–6854.
Kim, S., Ghafoor, K., Lee, J., Feng, M., Hong, J., Lee, D., Park, J., 2013. Bacterial inactivation in water, DNA strand breaking, and membrane damage induced by ultraviolet-assisted titanium dioxide photocatalysis. Water Res. 47, 4403–4411.
Kuo, D.H., Hsu, W.T., Yang, Y.Y., 2016. From the fluorescent lamp-induced bactericidal performance of sputtered Ag/TiO_2 films to re-explore the photocatalytic mechanism. Appl. Catal. B Environ. 184, 191–200.
Lee, J., Donahue, N.M., 2011. Secondary organic aerosol coating of synthetic metal–oxide nanoparticles. Environ. Sci. Technol. 45 (11), 4689–4695.
Leong, K.H., Gan, B.L., Ibrahim, S., Saravanan, P., 2014. Synthesis of surface plasmon resonance (SPR) triggered Ag/TiO_2 photocatalyst for degradation of endocrine disturbing compounds. Appl. Surf. Sci. 319, 128–135.
Li, T., Zhao, L., He, Y., Cai, J., Luo, M., Lin, J., 2013. Synthesis of g-C_3N_4/$SmVO_4$ composite photocatalyst with improved visible light photocatalytic activities in RhB degradation. Appl. Catal. B Environ. 129, 255–263.
Li, C., Hsieh, J.H., Cheng, J.C., Huang, C.C., 2014. Optical and photoelectrochemical studies on Ag_2O/TiO_2double-layer thin films. Thin Solid Films 570, 436–444.
Li, D., Zhu, Q., Han, C., Yang, Y., Jiang, W., Zhang, Z., 2015a. Photocatalytic degradation of recalcitrant organic pollutants in water using a novel cylindrical multi-column photoreactor packed with TiO_2-coated silica gel beads. J. Hazard. Mater. 285, 398–408.
Li, G., Nie, X., Chen, J., Jiang, Q., An, T., Wong, P.K., Zhang, H., Zhao, H., Yamashita, H., 2015b. Enhanced visible-light-driven photocatalytic inactivation of *Escherichia coli* using g-C_3N_4/TiO_2 hybrid photocatalyst synthesized using a hydrothermal-calcination approach. Water Res. 86, 17–24.
Mailler, R., Gasperi, J., Coquet, Y., Bulete, A., Vulliet, E., Deshayes, S., Zedek, S., Mirande-Bret, C., Eudes, V., Bressy, A., Caupos, E., Moilleron, R., Chebbo, G., Rocher, V., 2016. Removal of a wide range of emerging pollutants from wastewater treatment plant discharges by micro-grain activated carbon in fluidized bed as tertiary treatment at large pilot scale. Sci. Total Environ. 542, 983–996.
Mandal, S.S., Bhattacharyya, A.J., 2012. Electrochemical sensing and photocatalysis using Ag–TiO_2 microwires. J. Chem. Sci. 124, 969–978.
Méndez, D., Vargas, R., Borrás, C., Blanco, S., Mostany, J., Scharifker, B., 2005. A rotating disk study of the photocatalytic oxidation of p-nitrophenol on phosphorus-modified TiO_2 photocatalyst. Appl. Catal. B Environ. 166, 529–534.
Mohamed, M.M., Al-Sharif, M.S., 2013. Visible light assisted reduction of 4-nitrophenol to 4-aminophenol on Ag/TiO_2 photocatalysts synthesized by hybrid templates. Appl. Catal. B Environ. 142, 432–441.
Ng, T.W., Zhang, L., Liu, J., Huang, G., Wang, W., Wong, P.K., 2016. Visible-light-driven photocatalytic inactivation of *Escherichia coli* by magnetic Fe_2O_3-AgBr. Water Res. 90, 111–118.
Ortega-Gomez, E., Ballesteros Martin, M.M., Esteban Garcia, B., Sanchez Perez, J.A., Fernandez Ibanez, P., 2016. Wastewater disinfection by neutral pH photo-Fenton: the role of solar radiation intensity. Appl. Catal. B Environ. 181, 1–6.
Peng, W., Xu, Z., Luo, C., Zhao, H., 2015. Tailor-made core–shell CaO/TiO_2/Al_2O_3 architecture as a high-capacity and long-life CO_2 sorbent. Environ. Sci. Technol. 49 (13), 8237–8245.
Petronella, F., Rtimi, S., Comparelli, R., Sanjines, R., Pulgarin, C., Curri, M.L., Kiwi, J., 2014. Uniform TiO_2/In_2O_3 surface films effective in bacterial inactivation under visible light. J. Photochem. Photobiol. A Chem. 279, 1–7.
Pham, T.-D., Lee, B.-K., 2015. Photocatalytic comparison of Cu- and Ag-doped TiO_2/GF for bioaerosol disinfection under visible light. J. Solid State Chem. 232, 256–263.
Savio, A.K.P.D., Fletcher, J., Smith, K., Iyer, R., Bao, J.M., Hernández, F.R., 2016. Environmentally effective photocatalyst CoO–TiO_2 synthesized by thermal precipitation of Co in amorphous TiO_2. Appl. Catal. B Environ. 182, 449–455.
Shang, J., Zhang, Y., Zhu, T., Wang, Q., Song, H., 2011. The promoted photoelectrocatalytic degradation of rhodamine B over TiO_2 thin film under the half-wave pulsed direct current. Appl. Catal. B Environ. 102, 464–469.
Sofianou, M.V., Tassi, M., Psycharis, V., 2015. Solvothermal synthesis and photocatalytic performance of Mn^{4+}-doped anatase nanoplates with exposed {0 0 1} facets. Appl. Catal. B Environ. 162, 27–33.
Sukkasi, S., Terdthaichairat, W., 2015. Improving the efficacy of solar water disinfection by incremental design innovation. Clean Techn. Environ. Policy 17, 2013–2027.
Šuligoj, A., Štangar, U.L., Ristić, A., Mazaj, M., Verhovšek, D., Tušar, N.N., 2016. TiO_2–SiO_2 films from organic-free colloidal TiO_2 anatase nanoparticles as photocatalyst for removal of volatile organic compounds from indoor air. Appl. Catal. B Environ. 184, 119–131.
Teng, W., Li, X., Zhao, Q., Zhao, J., Zhang, D., 2012. In situ capture of active species and oxidation mechanism of RhB and MB dyes over sunlight-driven Ag/Ag_3PO_4 plasmonic nanocatalyst. Appl. Catal. B Environ. 125, 538–545.
Thanh-Dong, P., Lee, B.-K., 2015. Disinfection of *Staphylococcus aureus* in indoor aerosols using Cu-TiO_2 deposited on glass fiber under visible light irradiation. J. Photochem. Photobiol., A 307, 16–22.
Tian, G., Chen, Y., Bao, H., Meng, X., Pan, K., Zhou, W., Tian, C., Wang, J., Fu, H., 2012. Controlled synthesis of thorny anatase TiO_2 tubes for construction of Ag–AgBr/TiO_2composites as highly efficient simulated solar-light photocatalyst. J. Mater. Chem. 22, 2081–2088.
Viana, M.M., Mohallem, N.D.S., Miquita, D.R., Balzuweit, K., Silva-Pinto, E., 2013. Preparation of amorphous and crystalline Ag/TiO_2 nanocomposite thin films. Appl. Surf. Sci. 265, 130–136.
Wang, X., Lim, T., 2013. Highly efficient and stable Ag-AgBr/TiO_2 composites for destruction of *Escherichia coli* under visible light irradiation. Water Res. 47, 4148–4158.
Wang, X., Li, S., Yu, H., Yu, J., Liu, S., 2011. Ag_2O as a new visible-light photocatalyst: self-stability and high photocatalytic activity. European Journal]–>Chem. Eur. J. 17 (82), 7777–7780.
Wang, W., Ng, T.W., Ho, W.K., Huang, J., Liang, S., An, T., Li, G., Yu, J.C., Wong, P.K., 2013. $CdIn_2S_4$ microsphere as an efficient visible-light-driven photocatalyst for bacterial inactivation: synthesis, characterizations and photocatalytic inactivation mechanisms. Appl. Catal. B Environ. 129, 482–490.
Wang, P., Li, X., Fang, J., 2016. A facile synthesis of CdSe quantum dots-decorated anatase TiO_2 with exposed {0 0 1} facets and its superior photocatalytic activity. Appl. Catal. B Environ. 181, 838–847.
Xin, X., Xu, T., Yin, J., Wang, L., Wang, C., 2015. Management on the location and concentration of Ti^{3+} in anatase TiO_2 for defects-induced visible-light photocatalysis. Appl. Catal. B Environ. 176, 354–362.
Yu, J., Xiong, J., Cheng, B., Liu, S., 2005. Fabrication and characterization of Ag–TiO_2 multiphase nanocomposite thin films with enhanced photocatalytic activity. Appl. Catal. B Environ. 60 (3), 211–221.
Yu, H., Song, L., Hao, Y., Lu, N., Quan, X., Chen, S., Zhang, Y., Feng, Y., 2016. Fabrication of pilot-scale photocatalytic disinfection device by installing TiO_2 coated helical support into UV annular reactor for strengthening sterilization. Chem. Eng. J. 283, 1506–1513.
Zhu, L., He, C., Huang, Y., Chen, Z., Xia, D., Su, M., Xiong, Y., Li, S., Shu, D., 2012. Enhanced photocatalytic disinfection of *E. coli* 8099 using Ag/BiOI composite under visible light irradiation. Sep. Purif. Technol. 91, 59–66.
Zhu, Y., Yang, S., Cai, J., Meng, M., Li, X., 2015. A facile synthesis of Ag$x$$Au_{1-x}$/$TiO_2$ photocatalysts with tunable surface plasmon resonance (SPR) frequency used for RhB photodegradation. Mater. Lett. 154, 163–166.
Zielinska-Jurek, A., Kowalska, E., Sobczak, J.W., Lisowski, W., Ohtani, B., Zaleska, A., 2011. Preparation and characterization of monometallic (Au) and bimetallic (Ag/Au) modified-titania photocatalysts activated by visible light. Appl. Catal. B Environ. 101, 504–514.